INDO-UHF-CI Calculations of the Electronic Structure of Formaldehyde–Hydrogen Systems*

Kimiko MIZUTANI, Toyoo IZUMI,** and Shiro MATSUMOTO
Department of Chemistry, College of Science and Engineering, Aoyama Gakuin University, Chitosedai, Setagaya-ku, Tokyo 157

(Received October 29, 1976)

The electronic structures were calculated for the ground and several excited states of systems composed of a formaldehyde molecule and a hydrogen atom at various relative positions by means of an INDO-UHF-CI method, in order to elucidate the hydrogen-abstracting process of excited carbonyl compounds. The results were presented and discussed by means of the adiabatic potential energy curves, by means of configuration analysis using the various states of the non-interacting component species as reference, and by means of electron-density maps. The results showed in a concrete way that the process may proceed through an intermediate charge-transfer state, and the electron-density maps had features suggesting an attractive force acting on the positively charged hydrogen atom.

There have been increasing efforts to understand the mechanisms of chemical reactions in terms of the electronic structures of the molecular systems concerned.[1] The analyses have mostly been restricted to reactions between molecules in their ground states, although the principle may be the same for the cases when one or both of the partners are in excited states.

In the present work, electronic structures were calculated for systems composed of a formaldehyde molecule and a hydrogen atom at various relative positions in an attempt to get some insight into the nature of the hydrogen abstraction reaction of excited ketone molecules, as that reaction is one of the most clear-cut and best investigated chemical processes of excited states.[2] The process has, though, been described and discussed based only on the qualitative features of the electronic structures of the excited ketone molecules.[2,14c,15] For a more detailed understanding of the process, it seemed essential to compute the electronic structures of the combined system for a series of relative positions of the reactants. Since the calculation seemed, unfortunately, to be beyond the power of moderate computational facilities for real systems investigated experimentally, a model calculation was undertaken.

Ground and excited states of formaldehyde have been the subject of semiempirical calculations[3] of various precisions as well as of *ab initio* calculations.[4] The electronic states of the HCHO–H_2O system were calculated by Iwata and Morokuma.[5] In the case of the HCHO–H system, open shell or shells are involved in all the states, including the ground state. One way of treating the system would be a configuration interaction (CI) calculation using the configuration state functions (CSF's) constructed by the molecular orbitals (MO's) calculated for isolated HCHO plus an MO localized on the additional H atom. However, another method was attempted in this work; that is, the whole system was treated as a quasi-molecule by an SCF procedure. The method takes into account all the interactions between the components in a direct way at any internuclear distance. The resulting wavefunctions may be too complicated to be interpreted directly, but their expansions with the CSF's of the components (configuration analysis)[6] would help to grasp the characteristics of the states pictorially. As the RHF treatment will encounter the problem of orbital orthogonalization,[7] and as the wavefunction must be computed for a variety of geometries, the calculation was done by the INDO-UHF procedure[9] in order to obtain approximate wavefunctions without using too much computer time. Similar procedures have been used by several authors for similar purposes.[1d,1e] A fairly limited configuration interaction has been taken to improve the qualities of the excited states as well as of the ground state and to secure correct dissociation behavior[10b] of each state. In such a limited CI procedure, the SCF orbitals may be superior to the isolated HCHO and H orbitals for the state mainly composed of the ground-state configuration, as Brillouin's theorem[10c] states. For excited states, the situation was more subtle, but again the SCF orbitals seemed to be a better choice, as many terms cancelled each other out in the CI matrix element calculations. To visualize the results further, electron-density maps were drawn for some typical geometries. The conclusions obtained therefrom were in general agreement with those obtained by other methods of analysis; one interesting feature was that the maps were indicative of the direction of the force exerted on the approaching H atom.

Method of Calculation

The geometry of HCHO was taken to be planar (Fig. 1), and the dimensions were those given by the microwave analysis by Takagi.[8] They were fixed throughout this calculation. The position of the additional H atom will be defined below using the coordinate system given in Fig. 1. The method of INDO-UHF calculation was the same as that given in Ref. 9. The configuration interaction was confined to the 18 doublet CSF's*** resulting from the excitation of the π, n, and

---

* A part of this work was presented at the Symposium on Molecular Structure, Osaka, November 1975.

** Present address: Kyōei Keisan Center Co., Ltd., Setagaya-ku, Tokyo.

*** Quartet states resulting from ^{3}(HCHO)+H were not considered here, as they seemed to be of little importance in the photochemical process.

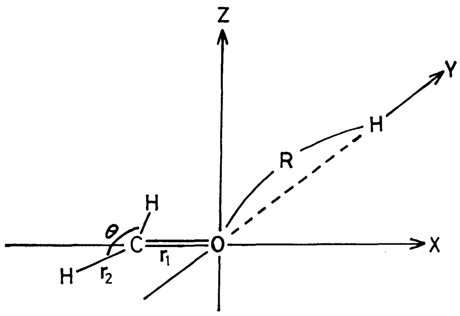

Fig. 1. Geometry of HCHO-H.
$r_1=1.2078$ Å, $r_2=1.1161$ Å, $\theta=116°31'$.

TABLE 1. LIST OF CONFIGURATION STATE FUNCTIONS

ψ_1		$(\pi)^2(\mathrm{n})^2(\mathrm{h})$
ψ_2		$(\pi)^2(\mathrm{n})(\mathrm{h})(\pi^*)^{\mathrm{a})}$
ψ_3		$(\pi)^2(\mathrm{n})(\mathrm{h})(\pi^*)^{\mathrm{a})}$
ψ_4		$(\pi)(\mathrm{n})^2(\mathrm{h})(\pi^*)^{\mathrm{c})}$
ψ_5		$(\pi)^2(\mathrm{h})(\pi^*)^2$
ψ_6		$(\pi)(\mathrm{n})^2(\mathrm{h})(\pi^*)^{\mathrm{c})}$
ψ_7	(BCT_1)	$(\pi)^2(\mathrm{n})(\mathrm{h})^2$
ψ_8		$(\pi)(\mathrm{n})(\mathrm{h})(\pi^*)^{2\ \mathrm{b})}$
ψ_9		$(\pi)(\mathrm{n})(\mathrm{h})(\pi^*)^{2\ \mathrm{b})}$
ψ_{10}	(BCT_2)	$(\pi)(\mathrm{n})^2(\mathrm{h})^2$
ψ_{11}	(CT_1)	$(\pi)^2(\mathrm{n})^2(\pi^*)$
ψ_{12}	(BCT_3)	$(\pi)^2(\mathrm{h})^2(\pi^*)$
ψ_{13}	(BCT_4)	$(\pi)(\mathrm{n})(\mathrm{h})^2(\pi^*)^{\mathrm{d})}$
ψ_{14}		$(\mathrm{n})^2(\mathrm{h})(\pi^*)^2$
ψ_{15}	(CT_2)	$(\pi)^2(\mathrm{n})(\pi^*)^2$
ψ_{16}	(BCT_5)	$(\pi)(\mathrm{n})(\mathrm{h})^2(\pi^*)^{\mathrm{d})}$
ψ_{17}	(CT_3)	$(\pi)(\mathrm{n})^2(\pi^*)^2$
ψ_{18}	(BCT_6)	$(\mathrm{n})^2(\mathrm{h})^2(\pi^*)$

a), b), c), d) These configuration state functions are independent-spin-state pairs.

h orbitals to the π^* virtual orbital. Here, the π, π^*, and n orbitals were named by analogy with the orbitals of isolated HCHO, and h denotes the orbital with its main component on the approaching H atom. These CSF's are summarized in Table 1, together with the numbering used below. The primitive UHF determinantal wavefunctions are not exact spin eigenfunctions, and the generation of exact state functions therefrom requires complicated procedures.[10] In view of the rather semi-quantitative nature of this work and various approximations already done in INDO calculation, no effort was made to spin-project the UHF determinantal wavefunctions; when their linear combinations were essential, as when three singly occupied orbitals existed, the following simple approximation was taken tentatively for the doublet wavefunctions. First, let it be assumed that the orbital functions for the α- and β-spins coincide as in RHF calculations. Corresponding to the excitation of an n electron in the ground configuration, Φ_0, to the π^* orbital, for example, there may result three independent determinantal wavefunctions: Φ_{n,π^*}, $\Phi_{\bar{\pi},\bar{\mathrm{n}}^*}$, and $\Phi_{\mathrm{h},\pi^*;\bar{\mathrm{n}},\bar{\mathrm{h}}}$ (Fig. 2). Two independent combinations of these determinants, which are exact doublets,[11] may be taken as

$$\Psi_{\mathrm{a}} = (\Phi_{\mathrm{n},\pi^*}+\Phi_{\bar{\mathrm{n}},\bar{\pi}^*})/\sqrt{2}, \tag{1}$$

$$\Psi_{\mathrm{b}} = (-\Phi_{\mathrm{n},\pi^*}+\Phi_{\bar{\mathrm{n}},\bar{\pi}^*}+2\Phi_{\mathrm{h},\pi^*;\bar{\mathrm{n}},\bar{\mathrm{h}}})/\sqrt{6}. \tag{2}$$

In the UHF case, orbital forms for α- and β-spins generally differ; however, if the differences are not too serious, Ψ_{a} and Ψ_{b} can be taken as representing approximately two doublet CSF's. For the estimation of the matrix elements of interaction between these CSF's, Slater's rule[12] was invoked, and the one- and two-electron integrals therein were again evaluated according to the prescription of the INDO method.

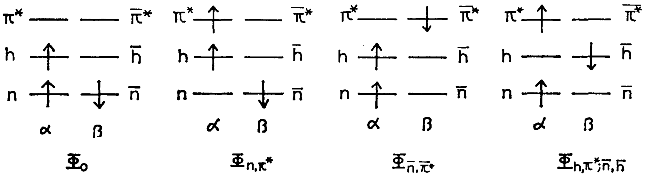

Fig. 2. Three independent arrangements of electrons resulting from nπ^* excitation.

Configuration analysis was done in essentially the same way as the original paper[6] with necessary adaptations to doublets. The reference states were those of a hypothetical system composed of non-interacting component species. Here, two combinations,

$$\Psi_{\mathrm{a}}^{\circ} = (\Phi_{\mathrm{n},\pi^*}^{\circ}+\Phi_{\bar{\mathrm{n}},\bar{\pi}^*}^{\circ})/\sqrt{2}, \tag{1'}$$

$$\Psi_{\mathrm{b}}^{\circ} = (-\Phi_{\mathrm{n},\pi^*}^{\circ}+\Phi_{\bar{\mathrm{n}},\bar{\pi}^*}^{\circ}+2\Phi_{\mathrm{h},\pi^*;\bar{\mathrm{n}},\bar{\mathrm{h}}}^{\circ})/\sqrt{6}. \tag{2'}$$

represent exact doublets, as the orbital functions for α- and β-spins coincide in this case. The superscript, o, on Φ means the reference state. On the other hand, the CSF's assumed above for the real system are contaminated by the quartet character. A third linear combination,

$$\Psi_{\mathrm{c}}^{\circ} = (-\Phi_{\mathrm{n},\pi^*}^{\circ}+\Phi_{\bar{\mathrm{n}},\bar{\pi}^*}^{\circ}-\Phi_{\mathrm{h},\pi^*;\bar{\mathrm{n}},\bar{\mathrm{h}}}^{\circ})/\sqrt{3},$$

is orthogonal to both $\Psi_{\mathrm{a}}^{\circ}$ and $\Psi_{\mathrm{b}}^{\circ}$ and represents a CSF quartet.[11] Thus, it would be appropriate to expand any state function, Ψ, in terms of this type of trio,

$$\begin{aligned}\Psi = \cdots &+ C_1(\Phi_{\mathrm{n},\pi^*}^{\circ}+\Phi_{\bar{\mathrm{n}},\bar{\pi}^*}^{\circ})/\sqrt{2}\\ &+ C_2(-\Phi_{\mathrm{n},\pi^*}^{\circ}+\Phi_{\bar{\mathrm{n}},\bar{\pi}^*}^{\circ}+2\Phi_{\mathrm{h},\pi^*;\bar{\mathrm{n}},\bar{\mathrm{h}}}^{\circ})/\sqrt{6}\\ &+ C_3(-\Phi_{\mathrm{n},\pi^*}^{\circ}+\Phi_{\bar{\mathrm{n}},\bar{\pi}^*}^{\circ}-\Phi_{\mathrm{h},\pi^*;\bar{\mathrm{n}},\bar{\mathrm{h}}}^{\circ})/\sqrt{3} + \cdots.\end{aligned} \tag{3}$$

Equation 3 may be rewritten as:

$$\Psi = \cdots + f_1\Phi_{\mathrm{n},\pi^*}^{\circ} + f_2\Phi_{\bar{\mathrm{n}},\bar{\pi}^*}^{\circ} + f_3\Phi_{\mathrm{h},\pi^*;\bar{\mathrm{n}},\bar{\mathrm{h}}}^{\circ} + \cdots, \tag{4}$$

with

$$\begin{aligned}f_1 &= C_1/\sqrt{2} - C_2/\sqrt{6} - C_3/\sqrt{3},\\ f_2 &= C_1/\sqrt{2} + C_2/\sqrt{6} + C_3/\sqrt{3},\\ f_3 &= 2C_2/\sqrt{6} - C_3/\sqrt{3}.\end{aligned} \tag{5}$$

The coefficients, f_1, f_2, and f_3 are determined by means of the Ψ function, $\Phi_{\mathrm{n},\pi^*}^{\circ}$, $\Phi_{\bar{\mathrm{n}},\bar{\pi}^*}^{\circ}$, and $\Phi_{\mathrm{h},\pi^*;\bar{\mathrm{n}},\bar{\mathrm{h}}}^{\circ}$ functions by the use of equations similar to those given in Ref. 6. The three Eqs. 5 are then solved to give

$$\begin{aligned}C_1 &= (f_1+f_2)/\sqrt{2},\\ C_2 &= (-f_1+f_2+2f_3)/\sqrt{6},\\ C_3 &= (-f_1+f_2-f_3)/\sqrt{3}.\end{aligned}$$

The C_3 coefficients are measures of the spin-contamination of the Ψ function.

Results and Discussion

Potential Curves and Configuration Analysis. The adiabatic potential curves obtained for several low-lying states are given in Figs. 3—5 for three modes of approach of the H atom. The results of configuration analysis along these curves are shown in Tables 2—6. In these figures, potential curves correlating to Ψ_5°, Ψ_7°, Ψ_8°, Ψ_9°, Ψ_{10}°, Ψ_{12}°, *etc.* for $R=\infty$ are not shown in order to avoid confusion. Each state, except for the one denoted as CT_1 in the figures, was found to dissociate rationally to an H atom and an HCHO molecule in its ground or in some of its excited states, which are shown beside each potential curve. The irreducible representation of each state is also indicated there. The CT symbol (charge transfer) is used here to denote states in which an electron in the h orbital is transferred to one of the empty orbitals of the HCHO component. As several different CT states arise, they are distinguished by subscripts, 1, 2, ···. They were found to dissociate to an H^+ and an $HCHO^-$ in its ground or various excited states. In the CT_1 state, the transferred electron occupies the LUMO π^* and has been found to play an important role in the chemical process under consideration. The BCT symbol (back charge transfer) indicates the states in which two electrons occupy the h orbital.

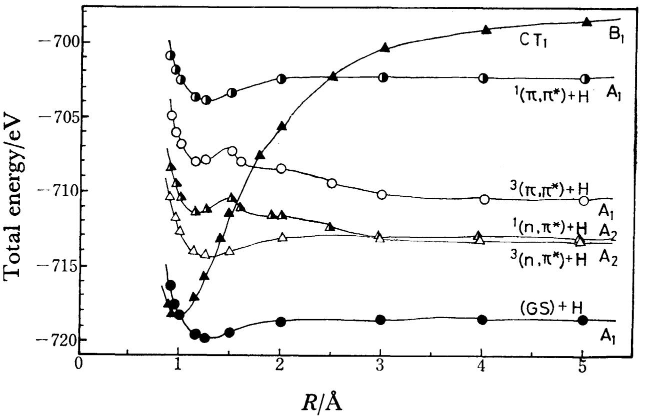

Fig. 3. Potential energy curves of ground and lower excited states of HCHO–H system; approaching H on X-axis. Beside each curve are given the states of components to which the state dissociates and the irreducible representation in C_{2v} point group.

When the H atom approaches along the X-axis (Fig. 3), the CT_1 curve drops sharply as R is reduced, but it merely crosses the lower potential curves. Even finite speed motions of the H atom will not cause transitions between these states. As a consequence, the H atom will not be attracted strongly by an $n\pi^*$ or $\pi\pi^*$ excited HCHO molecule in these geometries. A shallow minimum found in each potential curve at an R value of $\approx$1.2 Å is also seen in the ground-state potential curve; it might represent an attraction which is the cause of a stable ketyl radical formation from an H atom and an HCHO in the ground state. Another notable point in this nuclear configuration is that the potential curves of the $[^3(n\pi^*)+H]$ and $[^1(n\pi^*)+H]$ states closely approach at an R value of 2.84 Å, where the two states exchange characters rather abruptly, but continuously (Fig. 3 and Table 2). This is a case of pseudo-crossing,[13] and the transition between these adiabatic states may become possible by finite-speed motions of the H atom relative to the HCHO molecule. This observation is interesting because it seems to represent a mechanism by which singlet-triplet transitions of molecules are promoted through the formation of charge-transfer complexes with other species having odd electrons.

Table 2. Configuration analysis of $[^3(n\pi^*)+H]$ (H on X-axis)

R(Å)	ψ_2°	ψ_3°	ψ_8°	Total (%)
4.0	1.0	—	—	100
3.0	0.993	0.007	−0.003	98.7
2.848	0.896	0.420	−0.005	98.0
2.846	0.734	0.634	−0.004	98.5
2.844	0.536	0.840	−0.003	99.2
2.0	0.019	0.992	−0.003	98.4
1.5	0.022	0.958	−0.008	90.5
1.25	0.028	0.898	−0.016	80.7
1.15	0.039	0.866	−0.020	75.1
1.0	0.046	0.796	−0.021	63.1
0.95	0.046	0.751	−0.019	56.8
0.9	0.042	0.687	−0.014	47.6

$\psi_2^\circ=[^3(n\pi^*)+H]^\circ$, $\psi_3^\circ=[^1(n\pi^*)+H]^\circ$, $\psi_8^\circ=[^3(n\pi,\pi^*\pi^*)+H]^\circ$.

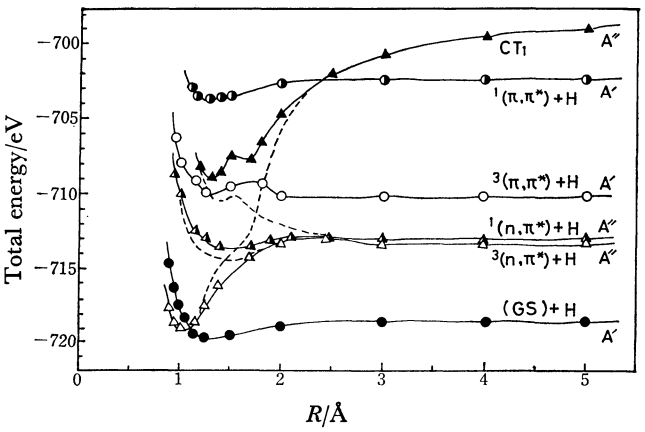

Fig. 4. Potential energy curves of ground and lower excited states of HCHO–H system; approaching H on Y-axis. Beside each curve are given the states of components to which the state dissociates and the irreducible representation in C_s point group.

When the H approaches along the Y-axis to the HCHO in the $^1(n\pi^*)$ or $^3(n\pi^*)$ excited state, the energy of the system decreases remarkably as a result of the strong configurational mixing with the CT_1 state (Fig. 4 and Table 3). The broken lines in Fig. 4 are intended to express these facts schematically. The transition to the ground state is, however, impossible in this mode of approach.

When the H atom is on the Z-axis, it is the $[^3(\pi\pi^*)+H]$ state which shows a marked decrease in energy as a result of the configurational mixing. The situation is

TABLE 3. CONFIGURATION ANALYSIS OF $[^3(n\pi^*)+H]$ (H ON Y-AXIS)

R(Å)	ψ°_2	ψ°_3	ψ°_{11}	ψ°_{12}	ψ°_{17}	Total (%)
4.0	0.999	—	−0.005	−0.014	0.001	100
3.0	0.997	0.008	−0.012	−0.024	0.003	99.4
2.4	0.785	0.600	−0.022	−0.055	0.005	97.9
2.0	0.004	0.967	−0.214	−0.033	0.028	93.8
1.7	0.242	−0.353	0.622	0.440	−0.151	79.0
1.5	0.099	−0.194	0.739	0.325	−0.191	73.7
1.25	−0.245	−0.162	0.704	0.244	−0.197	68.2
1.15	−0.176	−0.172	0.707	0.194	−0.202	64.1
1.0	−0.176	−0.189	0.678	0.185	−0.201	60.5
0.95	−0.151	−0.197	0.671	0.171	−0.191	58.7

$\psi^\circ_2=[^3(n\pi^*)+H]^\circ$, $\psi^\circ_3=[^1(n\pi^*)+H]^\circ$, $\psi^\circ_{11}=CT^\circ_1$
$\psi^\circ_{12}=BCT^\circ_3$, $\psi^\circ_{17}=CT^\circ_3$.

complicated here because of the abundance of states involved, but the results of configuration analysis may be summarized schematically as follows. The CT_1 state first interacts with $[^1(\pi\pi^*)+H]$ in the region of $R=$ 2.5—3.0 Å, and its character is transferred to the latter. The second state then interacts with $[^3(\pi\pi^*)+H]$ in the region of $R=2.2-1.3$ Å; the lower state acquires a CT_1 character, and its energy drops remarkably as R becomes smaller, until it reaches near that of the ground state, where a third pseudo-crossing to the latter state occurs. The lowest adiabatic state is seen to have a CT_1 character as the main one for $R\lesssim1.0$ Å. Another feature of these geometries is that the BCT_6 character seems to be an important cause of the energy decrease of the $[^3(\pi\pi^*)+H]$ state in the region of $R=3.0-2.2$ Å.

The importance of the charge-transfer type of intermediate states has frequently been suggested for quench-

TABLE 4. CONFIGURATION ANALYSIS OF $[^3(\pi\pi^*)+H]$ (H ON Z-AXIS)

R(Å)	ψ°_1	ψ°_4	ψ°_6	ψ°_{10}	ψ°_{11}	ψ°_{14}	ψ°_{17}	ψ°_{18}	Total (%)
4.0	—	0.996	0.002	−0.011	−0.048	0.001	0.002	−0.080	100
3.0	−0.001	0.857	0.063	−0.063	−0.269	0.021	0.014	−0.428	99.8
2.2	−0.004	0.510	0.266	−0.080	−0.508	0.081	0.048	−0.618	98.7
1.7	0.027	0.069	0.344	−0.050	−0.635	0.089	0.059	−0.298	63.0
1.5	0.121	0.200	0.384	−0.049	−0.711	0.064	0.048	−0.303	81.0
1.3	0.312	0.229	0.395	−0.004	−0.656	0.174	0.103	−0.323	88.3
1.15	0.521	0.259	0.337	0.121	−0.494	0.227	−0.071	−0.306	86.4
1.0	0.628	0.196	0.229	0.265	−0.319	0.269	−0.039	−0.156	75.5
0.95	0.675	0.244	0.232	0.287	−0.303	0.319	−0.076	−0.182	88.5

$\psi^\circ_1=[(GS)+H]^\circ$, $\psi^\circ_4=[^3(\pi\pi^*)+H]^\circ$, $\psi^\circ_6=[^1(\pi\pi^*)+H]^\circ$, $\psi^\circ_{10}=BCT^\circ_2$, $\psi^\circ_{11}=CT^\circ_1$, $\psi^\circ_{14}=[(\pi\pi,\pi^*\pi^*)+H]^\circ$, $\psi^\circ_{17}=CT^\circ_3$, $\psi^\circ_{18}=BCT^\circ_6$.

TABLE 5. CONFIGURATION ANALYSIS OF $[(GS)+H]$ (H ON Z-AXIS)

R(Å)	ψ°_1	ψ°_4	ψ°_6	ψ°_{10}	ψ°_{11}	ψ°_{14}	ψ°_{17}	ψ°_{18}	Total (%)
4.0	1.0	—	—	—	—	—	—	—	100
3.0	0.994	0.002	−0.010	0.022	0.003	0.029	−0.099	−0.002	100
2.0	0.969	0.004	−0.040	0.132	0.009	0.109	−0.159	−0.026	99.5
1.5	0.925	0.008	−0.043	0.270	0.057	0.132	−0.123	−0.028	96.8
1.25	0.817	0.054	−0.064	0.331	0.243	0.076	−0.064	0.078	86.1
1.15	0.691	−0.016	−0.118	0.331	0.399	0.027	0.044	0.095	77.2
1.0	0.475	−0.010	−0.171	0.304	0.545	0.021	0.070	0.152	68.4
0.95	0.436	−0.137	−0.189	0.266	0.555	−0.019	0.097	0.145	65.6
0.9	0.377	−0.218	−0.340	0.253	0.552	−0.079	0.158	0.149	73.1

$\psi^\circ_1=[(GS)+H]^\circ$, $\psi^\circ_4=[^3(\pi\pi^*)+H]^\circ$, $\psi^\circ_6=[^1(\pi\pi^*)+H]^\circ$, $\psi^\circ_{10}=BCT^\circ_2$, $\psi^\circ_{11}=CT^\circ_1$, $\psi^\circ_{14}=[(\pi\pi,\pi^*\pi^*)+H]^\circ$, $\psi^\circ_{17}=CT^\circ_3$, $\psi^\circ_{18}=BCT^\circ_6$.

TABLE 6. CONFIGURATION ANALYSIS OF $[CT_1]$ (H ON Z-AXIS)

R(Å)	ψ°_4	ψ°_6	ψ°_{10}	ψ°_{11}	ψ°_{12}	ψ°_{14}	ψ°_{17}	ψ°_{18}	Total (%)
5.0	—	—	—	1.00	—	—	—	—	100
4.0	0.048	−0.082	0.005	0.995	0.001	−0.023	−0.006	−0.003	99.9
3.4	0.146	−0.263	0.044	0.945	0.006	−0.068	−0.003	−0.025	98.2
3.0	0.250	−0.513	0.144	0.776	0.144	−0.120	0.021	−0.081	97.2
2.5	0.262	−0.865	0.077	0.231	0.231	−0.173	0.140	−0.157	95.2
2.0	−0.229	0.799	−0.210	0.140	−0.365	0.164	0.185	−0.085	96.3
1.8	−0.198	0.573	−0.333	0.144	−0.570	0.118	−0.089	0.238	90.7
1.7	−0.381	0.633	−0.219	−0.024	−0.123	0.256	−0.292	0.496	99.1
1.6	−0.400	0.652	−0.035	−0.026	0.058	0.286	−0.344	0.520	99.9
1.5	−0.495	0.385	−0.017	−0.155	0.022	0.409	−0.466	0.252	88.5

$\psi^\circ_4=[^3(\pi\pi^*)+H]^\circ$, $\psi^\circ_6=[^1(\pi\pi^*)+H]^\circ$, $\psi^\circ_{10}=BCT^\circ_2$, $\psi^\circ_{11}=CT^\circ_1$, $\psi^\circ_{12}=BCT^\circ_3$, $\psi^\circ_{14}=[(\pi\pi,\pi^*\pi^*)+H]^\circ$, $\psi^\circ_{17}=CT^\circ_3$, $\psi^\circ_{18}=BCT^\circ_6$.

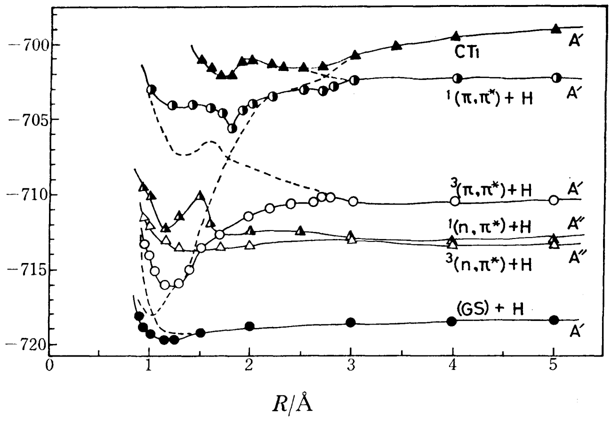

Fig. 5. Potential energy curves of ground and lower excited states of HCHO–H system; approaching H on Z-axis. Beside each curve are given the states of components to which the state dissociates and the irreducible representation in C_s point group.

Table 7. Quartet expansion coefficients of some state functions

a) $[^3(n\pi^*)+H]$ (H on X-axis)

R(Å)	2.845	2.4	2.0	1.5	1.25
C_3	0.0056	−0.0003	0.0009	0.0024	0.0011
C_3'	−0.00007	0.0005	−0.0021	−0.011	−0.019

b) $[^3(n\pi^*)+H]$ (H on Y-axis)

R(Å)	2.5	2.0	1.5	1.25
C_3	−0.0075	−0.012	−0.32	−0.32

c) $[^3(\pi\pi^*)+H]$ (H on Z-axis)

R(Å)	2.5	2.0	1.5	1.25
C_3''	0.025	0.059	0.32	0.25

C_3, C_3', and C_3'' are the coefficients in Eq. 3 for the $(\pi)^2(n)(h)(\pi^*)$, $(\pi)(n)(h)(\pi^*)^2$, and $(\pi)(n)^2(h)(\pi^*)$ configurations of the reference system respectively.

ing and photochemical redox processes,[14)] and potential curves have been deduced[14a)] to describe them in a general but semi-quantitative way. The present straightforward calculation yielded a more concrete picture of the process. One point of criticism that might affect the quantitative aspects of the results was, however, the spin-contaminations of the wavefunctions used. The C_3 coefficients were moderate for the X-approach, but took appreciable values at certain geometries for the Y- and Z-approaches (Table 7). This will considerably obscure the quantitative aspects of the C_1 and C_2 coefficients of the same configuration at those geometries. An inspection showed that the main contribution to the large values in Tables 7b and 7c came from the expansion of CT_1 CSF, and showed the necessity of at least a partial spin-projection in a more quantitative work.

Electron-density Maps. The chemical process could be perceived more visually through inspections of the electron-density maps. The electron-density distributions of the total valence electrons for the system of an HCHO in the ground state and of an H atom on the X-axis were not much different from that of an isolated HCHO, except for a slight electron density in the regions between the two components. This may be the cause of a shallow minimum seen in the [(GS)+H] curve of Fig. 3. The same was found to be true for the system of the $^3(n\pi^*)$ HCHO and the H atom on the X-axis, in which case charge-transfer cannot occur because of symmetry reasons.

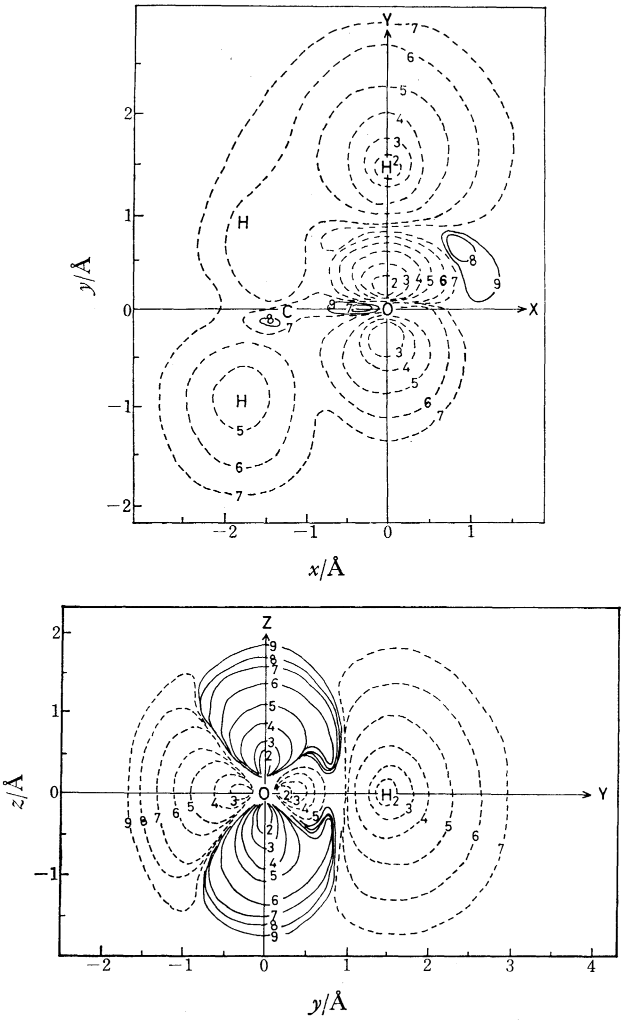

Fig. 6. Change in electron density upon $^3(n\pi^*)$ excitation; approaching H on Y-axis. Full lines indicate increase and broken lines decrease in electron density. The numbers 1, 2, ···, 9 beside the contours indicate electron density change of 2.0, 1.0, 0.5, 0.2, 0.05, 0.01, 0.002, 0.0005, and 0.0001 electrons/Å^3, respectively.
a) XY-plane, b) YZ-plane.

The electron density was also not much different from that of the isolated system with the H on the Y-axis when the HCHO component was in the ground state, but an essential change was seen when the HCHO was excited to the $^3(n\pi^*)$ state. The difference in the electron densities between the two states is shown in Fig. 6a. In most of the XY-plane, the electron densities are taken off perpendicularly to both sides of the plane upon excitation, whereas small regions of increased electron density appear near the O atom on the CO-axis and in the first quadrant. As there is only a weak attraction exerted on the H atom in the ground state, the separated charge upon excitation may be responsible

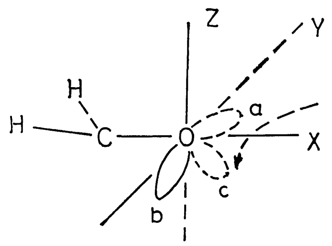

Fig. 7. Inferred path of H toward (nπ^*) excited HCHO in a quasi-static approach. a, b: Leaves of n orbital. c indicates O–H bond orbital in ketyl radical.

for determining the remarkable attraction exerted on the H in this nuclear configuration. One may see that the projection of the vector of the attraction force on the XY-plane is not toward the carbonyl oxygen, but toward a region which is an extension of the CO-axis, as may be seen in Fig. 6a. A similar contour map on the YZ-plane is given in Fig. 6b. The positively charged H atom is seen to be attracted by the negative charge generated on both sides of the XY-plane upon nπ^* excitation.

By reference to the results obtained above, one may guess the way the H atom is abstracted from a hydrogen donor by nπ^* excited HCHO. The excited state of HCHO is known to be bent. Let the two H atom of HCHO be above the XY-plane (Fig. 7). When the H being abstracted approaches along a path on the XZ-plane, no charge-transfer contribution may be expected to lower the potential energy of the system, just as in the cases shown in Figs. 3 and 5. The most favorable path of statical approach seems again to be nearly along a leaf (a in Fig. 7) of the n orbital at first, then gradually curving to the final place in the ketyl radical (at an end of c in Fig. 7). The electron-density increase may be more pronounced in the negative Z-direction than in the positive Z-direction, as compared with the pattern in Fig. 6b, as a result of the bent structure of HCHO. The attraction force on the positively charged H may be directed toward the region of the outweighted negative charge. In this case, a less symmetric nuclear arrangement will allow the transition from the CT$_1$ mixed state to the ground state at a potential curve crossing point similar to the one seen in Fig. 4.

From Fig. 5 it may seem that the $^3(\pi\pi^*)$ excited HCHO could also abstract hydrogen from a hydrogen donor approaching from the Z-direction if a non-adiabatic transition occurred between the potential curves of $[^3(\pi\pi^*)+\mathrm{H}]$ and $[(\mathrm{GS})+\mathrm{H}]$ around a geometry of $R\approx 1.1$ Å.

The present calculation does not seem to account for the fact[15] that carbonyl compounds with $^3(\pi\pi^*)$ as the lowest triplet have, in general, less reactivities toward hydrogen abstraction than those with $^3(\mathrm{n}\pi^*)$ as the lowest triplet. One explanation seems to be as follows. According to Slater's rule, the CI matrix element between two CSF's is calculated, if they are different in one spin-orbital pair, as the energy of the overlap density of the pair orbitals in the field generated by the nuclei and the electrons in the orbitals other than this pair. The CI matrix element between $[(\pi\pi^*)+\mathrm{H}]$ and CT$_1$ is, then, mainly determined by the overlap density between the π and the h orbital, whereas the matrix element between $[(\mathrm{n}\pi^*)+\mathrm{H}]$ and CT$_1$ is determined by that between the n and the h orbitals. The carbonyl compounds commonly used in the hydrogen abstraction reaction contain large conjugated π systems, and the overlap between π and h orbitals may be comparatively smaller than in the present case. The orbital overlap between n and h may be affected only slightly by the conjugation due to the local nature of the n orbital. In the carbonyl compounds with the lowest CT-triplet,[15] this effect may even become prominent.

References

1) a) H. Nakatsuji, *J. Am. Chem. Soc.*, **96**, 30 (1974); b) A. Igawa and H. Fukutome, *Prog. Theor. Phys.*, **52**, 115 (1974); c) K. Fukui, S. Kato, and H. Fujimoto, *J. Am. Chem. Soc.*, **97**, 1 (1975); d) K. Ohta, K. Yamaguchi, and T. Fueno, 2L20, 34th National Meeting of the Chemical Society of Japan, Hiratsuka, April (1976); e) S. Nagase and T. Fueno, *Bull. Chem. Soc. Jpn.*, **49**, 2920 (1976).

2) a) J. C. Dalton and J. N. Turro, *Ann. Rev. Phys. Chem.*, **21**, 499 (1970); b) G. Porter, "Reactivity, Radiationless Conversion and Electron Distribution in the Excited States," and N. C. Yang, "Photochemical Reactions of Ketones in Solution, the Hydrogen Transfer Reaction," in "Reactivity of the Photoexcited Organic Molecules," Interscience Publishers, New York (1967), p. 79, 145.

3) J. W. Sidman, *J. Chem. Phys.*, **27**, 429 (1957); F. L. Pilar, *ibid.*, **47**, 884 (1967).

4) J. L. Whitten and M. Hackmeyer, *J. Chem. Phys.*, **51**, 5584 (1969); R. J. Buenker and S. D. Peyerimhoff, *ibid.*, **53**, 1368 (1970); J. L. Whitten, *ibid.*, **56**, 5458 (1972); K. Tanaka, *Int. J. Quantum Chem.*, **8**, 981 (1974).

5) S. Iwata and K. Morokuma, *J. Am. Chem. Soc.*, **95**, 7563 (1973).

6) H. Baba, S. Suzuki, and T. Takemura, *J. Chem. Phys.*, **50**, 2078 (1969).

7) C. C. J. Roothaan, *Rev. Mod. Phys.*, **32**, 179 (1960); W. J. Hunt, T. H. Dunning, Jr., and W. A. Goddard III, *Chem. Phys. Lett.*, **3**, 606 (1969).

8) K. Takagi and T. Oka, *J. Phys. Soc. Jpn.*, **18**, 1174 (1963).

9) J. A. Pople and D. L. Beveridge, "Approximate Molecular Orbital Theory," McGraw-Hill Book Company, New York (1967).

10) H. F. Schaefer, III, "The Electronic Structure of Atoms and Molecules," Addison-Wesley Pub. Co., Reading (1972); a) p. 24, b) p. 148, c) p. 10.

11) R. Pauncz, "Alternant Molecular Orbital Method," W. B. Saunders Co., Philadelphia, Pa. (1967).

12) R. McWeeny and B. T. Sutcliff, "Method of Molecular Quantum Mechanics," Academic Press, New York (1969), p. 48.

13) D. R. Bates, "Atomic and Molecular Processes," Acad. Press, New York (1962), p. 608.

14) a) Y. Mori, *Bull. Chem. Soc. Jpn.*, **35**, 1584 (1962); b) H. Leonhardt and A. Weller, *Ber. Bunsenges. Phys. Chem.*, **67**, 791 (1963); c) G. Porter and P. Suppan, *Trans. Faraday Soc.*, **62**, 3375 (1966); d) A. Bjerre and E. E. Nikitin, *Chem. Phys. Lett.*, **1**, 179 (1967); e) G. Karl, P. Krauss, J. C. Polanyi, and I. W. M. Smith, *J. Chem. Phys.*, **46**, 244 (1967); f) E. Bauer, E. R. Fischer, and F. R. Gilmore, *J. Chem. Phys.*, **51**, 4173 (1969); g) G. H. Parsons, Jr. and S. G. Cohen, *J. Am. Chem. Soc.*, **96**, 2948 (1974).

15) G. Porter and P. Suppan, *Trans. Faraday Soc.*, **61**, 1664 (1965).